RELATIONSHIP BETWEEN OCULAR AXIAL LENGTH AND GANGLION CELL RESPONSES

A thesis presented to the graduate faculty of New England College of Optometry in partial fulfillment of the requirements for the degree of Master of Science

Simon Wong

May, 2025

RELATIONSHIP BETWEEN OCULAR AXIAL LENGTH AND GANGLION CELL RESPONSES

Simon Wong

This manuscript has been read and accepted by the
Thesis Committee in satisfaction with the
thesis requirement for the degree of Master of Science

5/11/2025
Date

DocuSigned by:
Fuensanta Vera-Diaz
1502BB240B7D484...
Fuensanta A. Vera-Diaz, OD, PhD, FAAO, FARVO
Graduate Faculty Advisor

DocuSigned by:
78A8AD972399447...
Athanasios Panorgias, MSc, PhD
Graduate Faculty Advisor

DocuSigned by:
Chris Taylor
8C96C99C286D4CA...
Christopher P. Taylor PhD
Thesis Committee Member

DocuSigned by:
Peter Bex
3E92398B6010477F...
Peter J. Bex, PhD
Thesis Committee Member

5/11/2025
Date

DocuSigned by:
78A8AD972399447...
Athanasios Panorgias, MS, PhD
Director of Graduate Studies

RELATIONSHIP BETWEEN OCULAR AXIAL LENGTH AND GANGLION CELL RESPONSES

Simon Wong

New England College of Optometry, 2025

ABSTRACT

Purpose: The progressive increase in ocular axial length (AXL), characteristic of myopia, has been associated with structural and functional changes in the retina. The specific retinal layer, or cells, associated with this mechanism still remains unclear. Retinal ganglion cells (RGCs) are an important neuron in the retinal highly involved in the visual process. Understanding visual processing and its relationship with RGC would further elucidate on the mechanism of axial elongation. This thesis investigates the relationship between AXL and ganglion cell responses using contrast sensitivity and electrophysiology tasks in a cohort of young adults with a range of AXL.

Methods: Different gaze-contingent contrast sensitivity tasks with stimuli that varied in chromatic and temporal frequencies characteristics were used to elicit responses from the three visual pathways (parvocellular, magnocellular, and koniocellular), at two peripheral eccentricities (6 and 10 deg from the fovea). Additionally, a Global-flash multifocal ERG (GmfERG) method with an induced component (IC) in its wavefront was used to assess inner retinal function.

Results: When using the achromatic 20 Hz flickering stimulus (associated with the magnocellular pathway), a significant decrease in peak spatial frequency (SFpeak) was

found with increasing in AXL at 6 deg (R^2 = 0.185, p = 0.018), whereas a significant decrease in SFpeak was found at 10 deg (R^2 = 0.213, p = 0.008). No significant changes were observed with the 6 deg (SFpeak R^2 = 0.001, p = 0.087; CSpeak R^2 = 0.002, p = 0.815; Acuity R^2 = 0.020, p = 0.456; AULCSF R^2 = 0.011, p = 0.580), or the 10 deg red-green (parvocellular) tasks (SFpeak R^2 = 0.006, p = 0.675; CSpeak R^2 = 0.062, p = 0.170; Acuity R^2 = 0.008, p = 0.630; AULCSF R^2 = 0.01, p = 0.586). There was also no significance with the 6 deg (SFpeak R^2 = 0.034, p = 0.330; CSpeak R^2 = 0.030, p = 0.360; Acuity R^2 = 0.032, p = 0.345; AULCSF R^2 = 0.034, p = 0.330), or the 10 deg koniocellular blue-yellow tasks (SFpeak R^2 = 0.046, p = 0.237; CSpeak R^2 = 0.001, p = 0.864; Acuity R^2 = 0.077, p = 0.126; AULCSF R^2 = 0.041, p = 0.267). Lastly, there was no significance for the GmfERG IC amplitude (Eccentricity-1 R^2 = 0.100, p = 0.098; Eccentricity-2 R^2 = 0.017, p = 0.510; Eccentricity-3 R^2 = 0.167, p = 0.028; Eccentricity-4 R^2 = 0.114, p = 0.338; Eccentricity-5 R^2 = 0.028, p = 0.167; Eccentricity-6 R^2 = 0.003, p = 0.287), or implicit time at any eccentricity with respect to AXL (Eccentricity-1 R^2 = 0.031, p = 0.356; Eccentricity-2 R^2 = 0.003, p = 0.776; Eccentricity-3 R^2 = 0.035, p = 0.187; Eccentricity-4 R^2 = 0.041, p = 0.202; Eccentricity-5 R^2 = 0.014, p = 0.119; Eccentricity-6 R^2 = 0.002, p = 0.248).

Conclusions: These results suggest that retinal functions are affected by axial elongation. The shift in peak spatial frequency with an increase AXL, a decrease at 6-6-degrees but increasing at 10-degrees retinal eccentricity, with an achromatic flickering stimulus, suggests this is possibly related to reorganization within the magnocellular visual pathway.

Table of Contents

List of Figures and Tables

1. Introduction

1.1. Myopia

Myopia is a common refractive error that is becoming increasingly prevalent worldwide at an alarming rate. According to a study by Holden et al. (2016), the global prevalence of myopia and high myopia is expected to increase from 1.4 billion in 2020 to 4.8 billion with nearly 1 billion considered to have high myopia by 2050. While the underlying biological mechanism for myopia development remains unclear, it is known that myopia is associated with an increase in axial length (AXL) due to the failure of the normal emmetropization process during ocular development. Several factors have been linked to the rapid rise in myopia prevalence seen in recent decades, including lifestyle changes and environmental factors such as prolonged near-work and reduced exposure to the outdoors (Alvarez-Peregrina et al., 2020; Baird et al., 2010; Pan et al., 2012; Wen et al., 2020).

This increase in the prevalence of myopia and high myopia is a major global health concern that can have significant impacts on an individual's quality of life (Rose et al., 2000). Even more importantly, myopia poses a high risk for various pathological complications, including myopic maculopathy, primary open-angle glaucoma, and retinal detachment, all of which can lead to blindness (Saw et al., 2005). There is also an added economic and financial burden placed on people with myopia, with the annual cost of treatment and prevention in China alone estimated to be $10.1 billion (Ma et al.,

2022). For all these reasons, myopia is now considered a disease (National Academies of Sciences, Engineering, and Medicine, 2024).

Previous animal studies have shown that myopia development likely occurs at a local level in the retina. This is supported by studies investigating optical defocus on chick (Schaeffel et al., 1988), monkey (Hung et al., 1995), and guinea pig (McFadden et al., 2004) models. This is further pointed out by Huang et al. (2022), who suggested that abnormal visual experiences cause changes in retinal cell activities, leading to myopic eye growth. Given the key role of retinal ganglion cells (RGCs) in the visual pathway, it is likely that RGCs may play an important role in the mechanism of myopia.

1.2. Retinal Ganglion Cells and Visual Pathway

RGCs are neurons in the retina that play a major role in visual processing and the transfer of information from the retina to the visual cortex (Kim et al., 2021). Their cell bodies are located in the ganglion cell layer of the retina, with axons that comprise the retinal nerve fiber layer. RGCs also have arbors that project into the inner plexiform layer, where they synapse with amacrine and bipolar cells (Kim et al., 2021; Yoonessi & Yoonessi, 2011). There are about 20 distinct types of RGCs in the human retina, including midget, parasol, and small-bistratified RGCs (Edwards et al., 2021; Kim et al., 2021). These different types of RGCs run parallel with each other in distinct pathways and layers to the primary visual cortex for further visual processing. Midget RGCs are associated with the parvocellular pathway and make up about 70% of RGCs. They have smaller receptive fields, which aid in the detection of form and spatial resolution. They

are sensitive to high spatial frequencies, low temporal frequencies, and red-green color vision. Parasol RGCs are associated with the magnocellular pathway and make up about 10% of RBCs. They respond rapidly to stimuli and have very large receptive fields compared to midget RGCs. They are sensitive to contrast and are also sensitive to achromatic low spatial frequencies and high temporal frequencies, which help detect motion, stereopsis, and depth (Al-Hashmi et al., 2011; Edwards et al., 2021; Kim et al., 2021; Yoonessi & Yoonessi, 2011). Small-bistratified RGCs are associated with the koniocellular pathway and make up about 8-10% of RGCs. They are structurally smaller than the midget GCs but have a wide field of input from different cells and are thought to be the basis for blue-yellow opponency (Al-Hashmi et al., 2011; Edwards et al., 2021; Kim et al., 2021; Yoonessi & Yoonessi, 2011). The roles and characteristics of these three major types of RGCs, which contribute to the visual pathways, require further study.

Previous studies have demonstrated that ocular diseases do not affect all the visual pathways equally. Glaucoma is an example of an ocular disease characterized by an acquired loss of RGCs and axons within the optic nerve, corresponding to progressive loss of vision (Dietze et al., 2025). The RGCs and corresponding visual pathways, however, are not affected equally, with studies showing that early glaucoma affects the magnocellular pathway first (Klistorner & Graham, 1999; Ye et al., 2024). The koniocellular pathway finding in glaucoma is less consistent but likely compromised as well (Klistorner & Graham, 1999; Ye et al., 2024). Short-wavelength automated perimetry(SWAP) uses a blue stimulus in a yellow background and has been shown to

monitor early and advanced glaucoma, diabetic macular edema, and possibly other neuro-ophthalmic disorders (Wild, 2001).

1.3. Contrast sensitivity

Measurements of chromatic and achromatic contrast sensitivity have long been used to assess underlying retinal function by isolating the distinct pathways (Kim et al., 2021; Leonova et al., 2003; Yoonessi & Yooness, 2011). Stimuli contain information that each distinct pathway may be sensitive to, such as an isoluminant red and green for the parvocellular pathway, violet/blue and greenish yellow for the koniocellular, and achromatic for the magnocellular pathway (Yoonessi & Yooness 2011). The stimuli can also have specific temporal and spatial frequency properties that may further isolate the three pathways. Al-Hashmi et al. (2011) noted that the magnocellular pathway determines contrast sensitivity over a broad range of temporal frequencies, with the parvocellular pathway contributing to mid to high spatial frequencies. In their first experiment, they used a variation of achromatic, red-green, or blue-yellow stimuli in Gabor patterns with low spatiotemporal frequencies to maximize the contrast sensitivity of the three pathways. These were done in the same retinal location and did not compare across retinal eccentricities. It is essential to note, however, that although the different pathway cells are tuned to distinct spatial frequencies, there is considerable overlap in the range of spatial frequencies to which they are sensitive (Edwards et al., 2021). Each cellular pathway differs in its temporal sensitivity, with the magnocellular

pathway extending up to 30 Hz, while the parvocellular and koniocellular pathways are closer to 10-20 Hz (Al-Hashmi et al., 2011; Edwards et al., 2021).

An increase in contrast sensitivity has been noted in myopes compared to emmetropes in the parafoveal and mid-peripheral regions of the superior and inferior visual fields (Xu et al., 2022). On the other hand, fovea, on-axis contrast sensitivity may be reduced in myopia (Stoimenova, 2007). This could be further evidence of how peripheral contrast sensitivity affects emmetropization, leading to myopia progression. Receptive fields of retinal neurons are what is responsible for detecting contrast. RGCs play a crucial role in detecting contrast with their center-surround receptive fields. In myopia, particularly with axial elongation, the spatial organization and density of RGCs may be altered leading to a change in receptive field function. These changes could potentially reduce contrast sensitivity and electrophysiological responses. All this information is used in this thesis to create visual stimuli to isolate the distinct visual pathways for varying refractive errors.

1.4. Electroretinogram

Electroretinograms (ERGs) are a type of electrophysiological test that measures and assesses the biopotential of neurons in the retina. It achieves this by placing an electrode in contact with the eye while presenting various types of flashes and stimuli to elicit neuronal responses. The most common ERG test is the full-field ERG, which sums all electrical activity across the retina. While this is useful in certain cases, it can miss relatively large defects and does not give topographic information (Hood et al., 2003).

The multifocal electroretinogram (mfERG) typically utilizes 63 or 103 hexagonal focal areas of stimulation, flashed in a pseudorandom sequence, to provide topographic information and localize retinal activity (Hoffmann et al., 2021).

The global-flash mfERG (GmfERG) is a modified mfERG paradigm where an additional periodic full-field “global” flash frame is added to the pseudorandom sequence. This first-order kernel waveform contains two components, the direct component (DC) and the induced component (IC) (Shimada et al., 2005). The DC mainly originates from the outer retinal cells in response to a focal flash, and the induced component (IC), is an adaptive effect from the global flash and is dominated by inner retina function (Shimada et al., 2005; Fung et al., 2021; Chu et al., 2008). Previous studies have used the GmfERG to demonstrate that the retina can locally differentiate between different types of defocus induced by ophthalmic lenses.(Fung et al., 2021; Ho et al., 2012; Turnbull et al., 2020). These studies using hyperopic and myopic defocus to assess retinal function and designed to imitate the visual environment have shown mixed results, with both an increase and decrease in the IC amplitude with increased myopic defocus (Ho et al., 2012a; Ho et al., 2012b; Turnbull et al., 2020).

2. Specific Aims

The overall objective of my MS studies is to further our understanding of the relationship between AXL and the responses of ganglion cells in the human retina. I will evaluate this by performing both electrophysiological and psychophysical tests while examining different retinal eccentricities. For this, the specific aims of my project are:

Specific Aim-1: To investigate the relationship between AXL and peripheral CSF.

For this aim, we will test a group of young adults with a wide range of AXLs on:

- CSF at various locations in the periphery with various chromatic and temporal variables, using custom MATLAB programs.
- Ocular biometry using an optical biometer.

We hypothesize that subjects with longer AXL will show

(1) *a decrease in the high spatial frequency cut-off of the peripheral CSF.*

(2) *a decrease in peak spatial frequency of the peripheral CSF.*

Specific Aim-2: To investigate the relationship between AXL and ganglion cell responses as measured by a GmfERG protocol.

For this aim, we will test a group of young adults with a wide range of AXLs on:

- A GmfERG under photopic conditions with a Veris multifocal ERG system.
- Ocular biometry using an optical biometer.

We hypothesize that subjects with longer AXL will show:

(1*) a decrease in amplitude for the induced component (IC) of the GmfERG.*

(2) *an increase in implicit time for the IC of the GmfERG.*

3. Methods

This cross-sectional study is part of a larger study titled *Relationship between Axial Length and Retinal* Structure *and Function,* which aims to evaluate and measure the cellular structure and function of photoreceptors, bipolar cells, horizontal cells, amacrine cells, and ganglion cells, as well as visual performance in a group of healthy young adults. The procedures described here pertain only to the ganglion cells study, the topic of my thesis.

3.1. Subjects

Participants were young adults with healthy eyes and vision recruited from the New England College of Optometry (NECO) population, including students, faculty, and staff. The specific criteria for inclusion and exclusion were:

- Inclusion criteria:
    - Over the age of 18 and under the age of 32 years.
    - Emmetropes (spherical equivalent, SE, OD between +0.75 and -0.25D and CYL within 0.75DC).
    - Myopes (SE OD between -0.50 and -7.00D and CYL within 2.50DC).
    - Hyperopes (SE OD between +1.00 and +5.00D and CYL within 2.50DC).
    - Best corrected LogMAR VA = 0.0 (20/20 equivalent) or better in each eye.
- Exclusion criteria:

- History of ocular surgery, including extraocular muscle surgery for strabismus, or ocular disease that may have resulted in visual consequences.
- Strabismus or near vision binocular anomalies (other binocular vision anomalies may be included).
- History of orthokeratology or recent wear of rigid gas permeable contact lenses (within the past 14 days).
- Using medication (ocular or systemic) that may affect their vision.
- History of allergy to any eye drops.
- Pregnant or nursing.
- History of seizures or diagnosis of epilepsy.

Due to the nature of this study, to investigate the relationship between AXL and a variety of electrophysiological and psychophysical tasks, it is important to have a representative and roughly uniform distribution of AXLs among the participating individuals. Most of the study population consisted of students from the New England College of Optometry (NECO), who are not likely to know their AXL; thus, recruiting subjects based on their AXL is difficult. However, in two previous studies that measured AXL in NECO students (Hogue, La, and Taylor, 2019-2021), the mean AXL of those samples was 24.86 mm, with a standard deviation of 1.52 mm; both samples showed modest negative skewness (Hogue, La, and Taylor, 2021).

3.2. Study Protocol

This study was part of a larger study assessing the different retinal layers and cells with respect to AXL. My other colleagues in the OD/MS program (Rachel Harmon, Raviv Katz, Srinivas Srirangam) also perform a combination of psychological and electrophysiological tasks on the same patient population separated into 4 visits which are spaced out about 7 ± 3 days. The Visits relevant to my study are Visit 1 and Visit 3.

3.3. First Visit (Visit 1)

Following an explanation of the purposes of the study, the subject was asked to read the Informed Consent Form (ICF) and ask the investigator any questions they may have. The investigator ensured that the procedures and purposes had been clearly understood by the subject and any questions were answered. Once the ICF was signed, a de-identifier form was used to assign a study number to the subject. This study number, with no identifiable information, was used from that point forward.

At this visit, a vision screening was then performed to determine the subject's eligibility. The vision screening included:

- Comprehensive medical and ocular history.
- Lensometry of habitual glasses.
- Habitual distance and near visual acuity on each eye and both eyes, using a computerized logMAR chart.
- Habitual estimated cover test for distance and near.
- Near point of convergence using an accommodative target.

- Counting fingers confrontation fields in each eye.
- Extraocular muscle testing.
- Pupil evaluation, including measures of pupil sizes under dim, near, and bright conditions.
- Monocular estimation method (MEM) to measure the accommodative accuracy.
- Objective refraction with static retinoscopy and with a WAM open-field autorefractor (WAM-5500, Grand Seiko, Japan), to determine the spherical equivalent (SE) refractive correction in each eye.
- If the habitual distance VA was worse than 0.0 logMAR, or if the autorefractor results were more different than 0.50D from the subject's habitual glasses, a subjective refraction with binocular balance was also conducted to determine best refraction..
- Anterior ocular health evaluation using a slit lamp to determine the health of the ocular media.
- Intraocular pressure (IOP) with a rebound tonometer (Icare IC200; TiolatOy, Inc., Finland)
- Ocular biometry measurements using an optical biometer (Lenstar LS900, Haag-Streit, Switzerland). Five measurements were taken from each eye to obtain: AXL, central corneal thickness (CCT), anterior chamber depth (ACD), lens thickness (LT), and keratometry (K).

My colleague who tested subjects in this visit also used psychophysical task to measure responses from ON-Bipolar cells.

3.4. Second Visit (Visit 3)

Subjects were asked to return for a second visit within 10 days (± 3 days) at around the same time of the day (± 2 hours). At the beginning of this second visit, the investigators confirmed that no changes in ocular health had happened since the previous visit and they repeated the following vision tests: distance visual acuity of the right and left eyes, as described above, and anterior segment slit lamp examination, including Van Herick angle grading. The following experimental tests were performed at this visit:

A. Contrast sensitivity with chromatic and temporal modulation

Subjects performed a CSF task twice, once with the stimuli located at 6 degrees from the fovea and a second time with the stimuli at 10 degrees in the periphery, both under photopic conditions. Only the right eye was tested with the left eye occluded. The viewing distance for this task was 160 cm, which was the furthest distance the monitor size allowed, and the stimuli were presented on a screen subtending 48.09 degrees of visual angle.

The stimuli consisted of Gabor patches with a sine-wave luminance grating (Figure 1) of varying contrast and spatial frequency. Specific chromaticity and spatial frequencies were selected to activate each of the three retino-cortical pathways: (1) an achromatic grating contrast-reversing at 20 Hz was used to stimulate the magnocellular pathway (Edwards et al., 2021); (2) a static, 0 Hz, red-green stimulus grating was used to stimulate the parvocellular pathway (Edwards et al., 2021); and (3) a static, 0 Hz, blue-yellow stimulus grating was used to stimulate the koniocellular pathway (Edwards

et al., 2021). We utilized a custom program created in MATLAB by Dr. Peter Bex (Northeastern University) to measure the full CSF at two peripheral retinal locations: 6 degrees (with stimuli spanning between 4 and 8 degrees eccentricity) and 10 degrees (with stimuli spanning between 8 and 12 degrees eccentricity). The CSF was obtained using a modified staircase method (Bex).

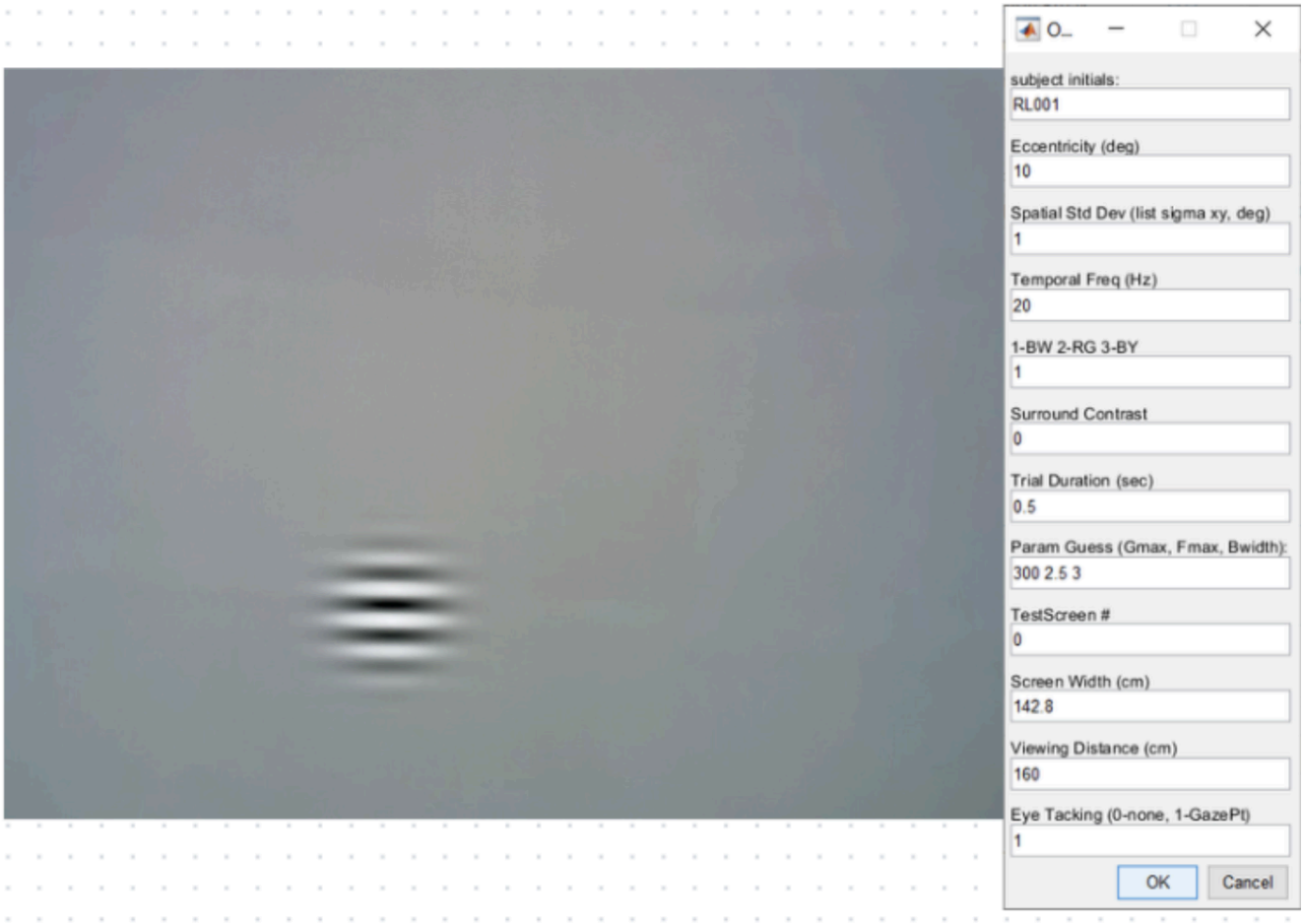

Figure 1. *Sample of the peripheral psychophysical task. Black-white stimulus centered at 10 degrees visual angle (spanning 8 to 12 degrees) with a 20 Hz flicker.*

For the peripheral contrast sensitivity tasks, as shown in Figure 1, an eye tracker (Gazepoint 3, Canada) was used to ensure central fixation and, therefore, the exact

presentation of the stimuli at the desired eccentricity. The peripheral Gabor patch only appeared when the subject fixated on the central fixation cross. The stimuli appeared randomly at one of eight locations: 0 °, 45 °, 90 °, 135 °, 180 °, 225 °, 270 °, or 315 ° from fixation. Subjects were asked to identify the location at which the stimulus appeared using a mouse click.

B. Global-Flash Multifocal ERG (GmfERG)

The GmfERG is an established mfERG protocol that provides information about both the inner and outer retina. The GmfERG was recorded in this study using the FDA-approved VERIS (Visual Evoked Response Imaging System, EDI Inc., Redwood City, CA, USA) multifocal ERG system. Subjects first had their pupils dilated to ≥ 7 mm diameter using 2gtt 0.5% tropicamide in their right eye. Following dilation, a Dawson, Trick, and Litzkow (DTL, Diagnosys LLC, Lowell, MA, USA) silver-nylon electrode was placed in contact with the right inferior bulbar conjunctiva and secured using adhesive pads on the lateral and nasal canthi. A ground skin electrode (3M Red Dot; 3M Corp, MN, USA) was secured on the forehead, and a reference electrode (Ambu neuroline 700, Ballerup, Denmark) was placed on the ipsilateral temple of the tested eye after properly preparing the skin. Impedance was checked and kept below 5 kΩ

The stimulus was presented through an FMS III EDI stimulator (Electro-Diagnostic Imaging, Milpitas, CA, USA), with an LCD micro display viewed through an optical system. The FMS III stimulator features an integrated refractor that provides correction of spherical refractive error from -8.00 to +6.00 diopters (D). The

optical system also compensates for stimulus minification or magnification to ensure constant stimulus size regardless of the observer's refractive error and consistent stimulus eccentricities. The stimulator was first aligned with the subject's pupil. The subject was then asked to self-adjust a knob until the focusing target, a red cross, was in sharp focus before recording GmfERG.

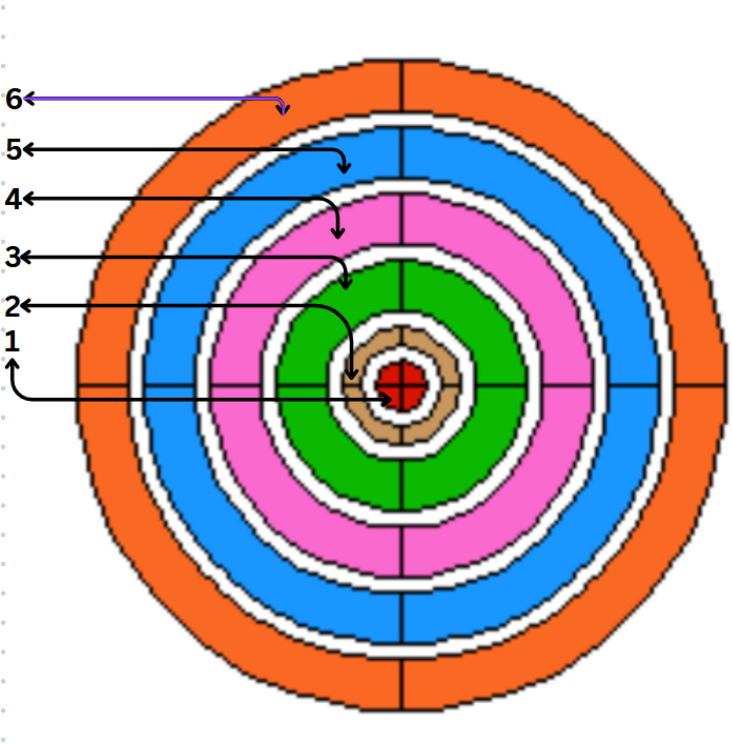

Figure 2. *The Global-Flash Multifocal ERG (GmfERG) stimulus. Stimulus consisted of concentric rings split into quadrants, adjusted to assess both foveal and mid-peripheral responses at 0-2º, 2-4º, 4-8º, 8-12º, 12-16º, and 16-20º eccentricities.*

Although the stimulator lacks astigmatic adjustment, previous studies have demonstrated that response amplitudes and latencies remain unaffected by astigmatic defocus (Turnbull et al., 2020). The stimulus consisted of concentric rings split into quadrants adjusted to assess both foveal and mid-peripheral responses at 0-2º, 2-4º, 4-8º, 8-12º, 12-16º, and 16-20º, totaling 24 arcs, as shown in Figure 2. These locations were chosen to allow comparison of the ERG and psychophysical data in the same zones of interest. The background was kept at a constant luminance of 75 cd/m^2.

Using the GmfERG protocol, we were able to extract the amplitude and implicit time of bipolar cells and ganglion cells by analyzing the different features of the recorded waveform, as shown in Figure 3.

3.5. Data Processing and Analysis

Global-flash mfERG responses were grouped into the six concentric rings for analysis, while the peak sensitivity and high spatial frequency cut-off of each CSF at each retinal location were used for analysis. As shown in Figure 3. The DC amplitude and implicit time were measured from the first largest peak, which was located at approximately 25-35 ms. The IC amplitude was calculated as the absolute sum of the second largest peak, occurring at around 50-60 ms, to the last largest trough, which occurred at around 60-65 ms.

Shapiro-Wilk tests were used to check for normality of the data ($p > 0.05$). Pearson's correlation or Spearman's rank correlation was used to test for correlation with AXL, depending on whether the distribution was normally distributed or not. Alpha

was set to be 0.05. Using Bonferroni correction for multiple comparison between the 6- and 10-degree stimulus we adjusted alpha to 0.025.

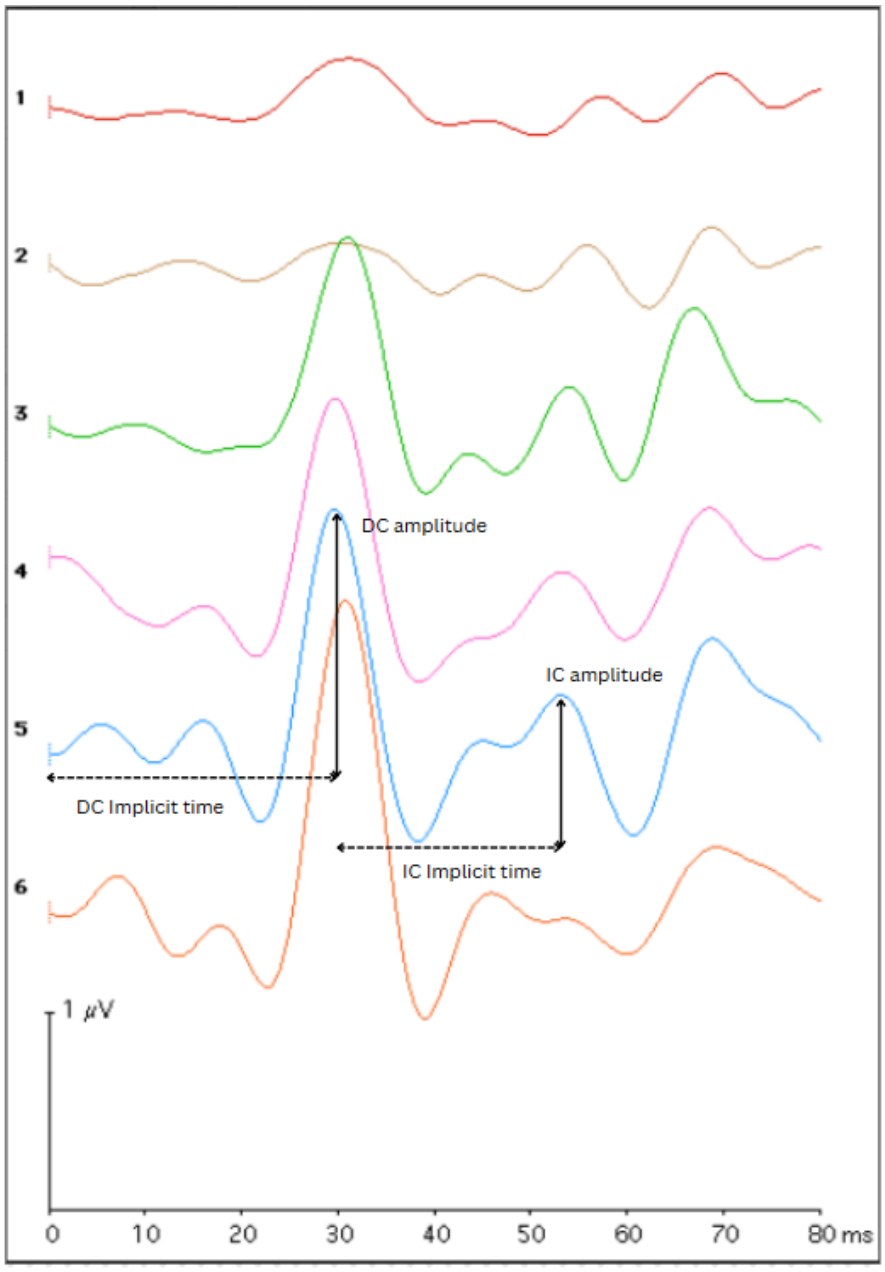

Figure 3. *Sample Global-Flash Multifocal ERG (GmfERG) waveforms. From top to bottom are Rings 1 to Ring 6 with the DC and IC amplitude and implicit time shown.*

4. Results

Recruitment took place between August 17, 2023, and July 20, 2024. Our subjects were recruited from the NECO population. A total of 37 participants were enrolled, with 36 participants completing all four visits. The average age of the 36 participants was 25.00 ± 2.22 years (Table 1). The mean AXL was 24.97 ± 1.17 mm.

Characteristics	Mean ± SD	Range
Age (years)	25.00 ± 2.22	22 - 32
Intraocular pressure (IOP, mmHg)	15.11 ± 2.39	10 - 20
Spherical Equivalent Habitual Rx (SEh, D)	-3.04 ± 2.49	(-6.75) - 2.00
Spherical Equivalent Autorefraction (SEa, D)	-3.11 ± 2.30	(-6.88) - 1.15
Axial Length (mm)	24.97 ± 1.17	22.50 - 27.51
Central Corneal Thickness (um)	542.11 ± 26.85	487 - 597
Anterior Chamber Depth (mm)	3.54 ± 0.35	2.83 - 4.18

Table 1. *Total demographic characteristics of the participating 36 subjects.*

A total of 30 subjects (Average age 22 ± 4.93 years, SE -3.08 ± 2.41 D, AXL 24.95 ± 1.23 mm) completed the psychophysical tasks at 6 deg, and 32 subjects (Average age 25 ± 4.86 years, SE -3.58 ± 2.41 D, AXL 25.32 ± 1.19 mm) completed the task at 10 deg eccentricity. The other subjects either could not complete the task or there was an issue with the gaze tracker, and the data was therefore not useful. The GmfERG had a total of 29 subjects (Average age 25 ± 2.25 years, SE -2.84 ± 2.55 D, AXL 25.07 ± 1.21 mm) with completed data, with 8 subjects either with incomplete visits or had issues with the electrode, leading to non-usable data.

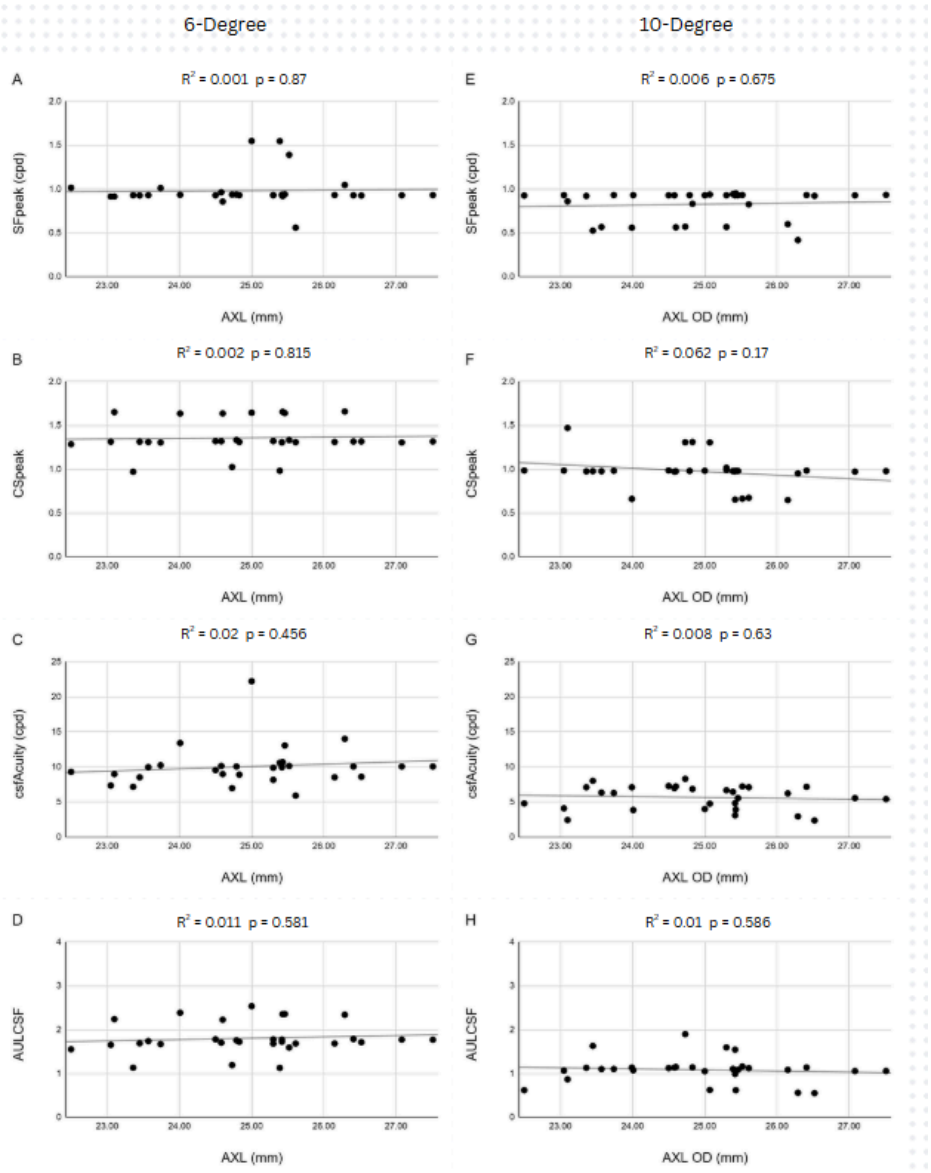

Figure 4. *Peripheral Red-Green contrast sensitivity task results. Associated with the parvocellular pathway, for the targets at 6 and 10 degrees visual angle. The peak spatial frequency (A and E), peak contrast sensitivity (B and F), Acuity (C and G), and AULCSF (D and H) plotted against axial length (mm).*

Figure 4 shows the psychophysical task of the red-green stimulus centered at 6 and 10 degrees retinal eccentricity, with peak spatial frequency (SFpeak, cpd), peak contrast sensitivity (CSpeak), Acuity (Acuity, cpd), and area under the log contrast sensitivity (AULCSF) plotted against AXL. The stimulus centered at 6 degrees found no statistically significant correlation between AXL and SFpeak (R^2 = 0.001, p = 0.087), CSpeak (R^2 = 0.002, p = 0.815), csfAcuity (R^2 = 0.02, p = 0.456), or AULCSF (R^2 = 0.011, p = 0.58). The stimulus centered at 10 degrees found no statistically significant correlation between AXL and SFpeak (R^2 = 0.006, p = 0.675), CSpeak (R^2 = 0.062, p = 0.17), Acuity (R^2 = 0.008, p = 0.63), or AULCSF (R^2 = 0.01, p = 0.586).

Figure 5 shows the psychophysical task of the Black-White stimulus centered at 6 and 10 degrees retinal eccentricity with SFpeak (cpd), CSpeak, csfAcuity (cpd), and AULCSF plotted against AXL. The stimulus centered at 6 degrees found statistical significance in the correlation of AXL with SFpeak (R^2 = 0.185, p = 0.018), with longer AXL showing reduced peak spatial frequency. There was no statistically significant correlation between AXL and CSpeak (R^2 = 0.009, p = 0.618), Acuity (R^2 = 0.151, p = 0.034), or AULCSF (R^2 = 0.021, p = 0.444). The stimulus centered at 10 degrees found a significant correlation between AXL and SFpeak (R^2 = 0.213, p = 0.0077), with longer AXL showing reduced peak spatial frequency. There was no statistically significant correlation between AXL and CSpeak (R^2 = 0.009, p = 0.605), Acuity (R^2 = 0.006, p = 0.675), or AULCSF (R^2 = 0.016, p = 0.492).

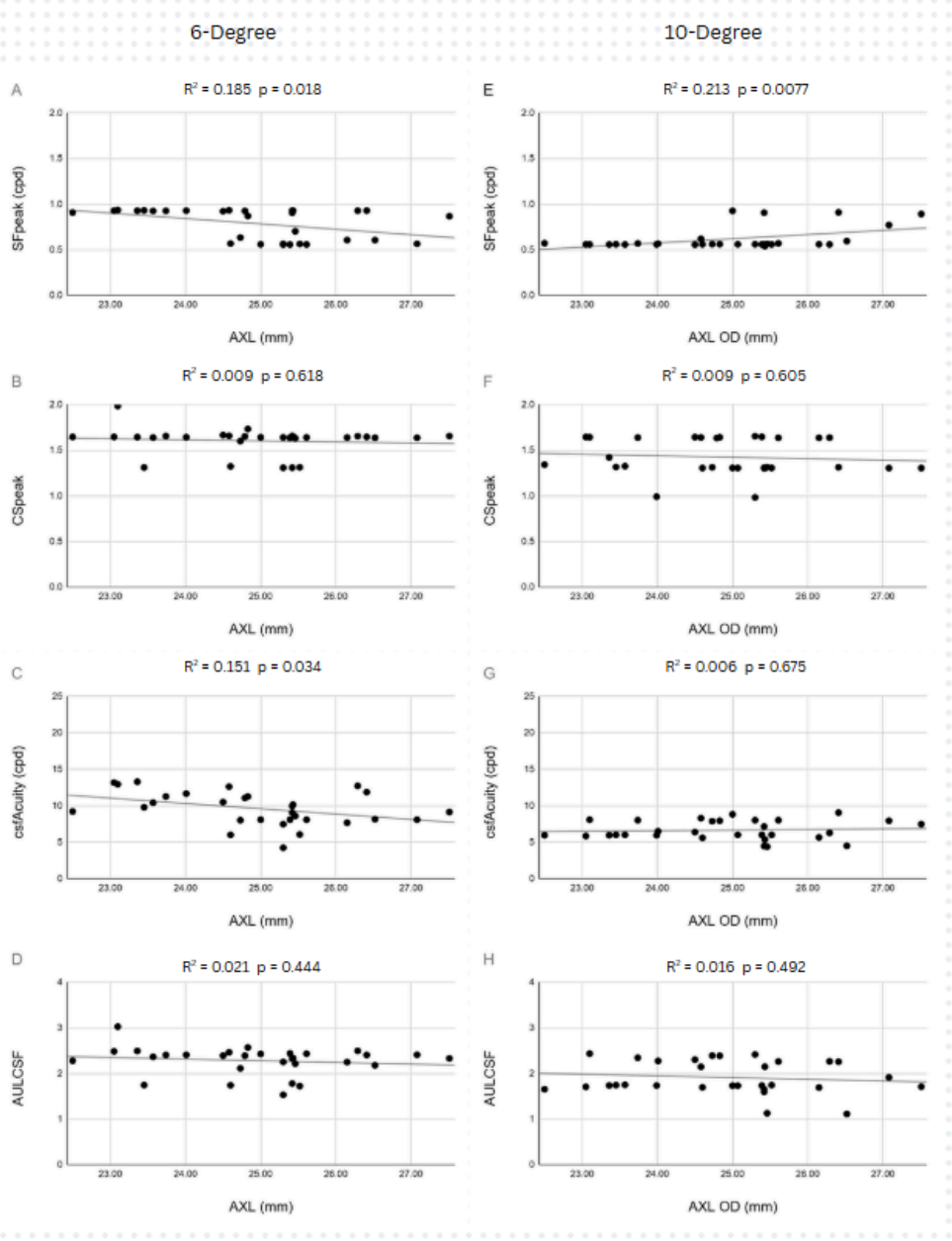

Figure 5. *Peripheral Black-White contrast sensitivity task results. Associated with the magnocellular pathway, with targets at 6 and 10 degrees visual angle. The 6-degree centered stimulus peak spatial frequency (A and E), peak contrast sensitivity (B and F), Acuity (C and G), and AULCSF (D and H) plotted against axial length (mm).*

Figure 6 shows the psychophysical task of the Blue-Yellow stimulus, centered at 6 and 10 degrees of retinal eccentricity, with SFpeak (cpd), CSpeak, Acuity (cpd), and AULCSF plotted against AXL. The stimulus centered at 6 degrees found no statistically significant correlation between AXL and SFpeak (R^2 = 0.034, p = 0.33), CSpeak (R^2 = 0.03, p = 0.36), Acuity (R^2 = 0.032, p = 0.345), or AULCSF (R^2 = 0.034, p = 0.33). The stimulus centered at 10 degrees found no statistically significant correlation between AXL and SFpeak (R^2 = 0.046, p = 0.237), CSpeak (R^2 = 0.001, p = 0.864), csfAcuity (R^2 = 0.077, p = 0.126), or AULCSF (R^2 = 0.041, p = 0.267).

Figure 7 shows the IC Amp (μV) and IC Imp (ms) of the GmfERG at eccentricity 1-6 (0-20 degrees) plotted against AXL. For eccentricity 1 (0-2 degrees), there was no statistically significant correlation found between AXL and the IC Amp (R^2 = 0.1, p = 0.098) or IC Imp (R^2 = 0.031, p = 0.356). For eccentricity-2 (2-4 degrees), there was no statistically significant correlation between AXL and the IC Amp (R^2 = 0.017, p = 0.51) or IC Imp (R^2 = 0.003, p = 0.776). For eccentricity-3 (4-8 degrees), there was no statistically significant correlation between AXL and the IC Amp (R^2 = 0.167, p = 0.028), or IC Imp (R^2 = 0.035, p = 0.187). For eccentricity-4 (8-12 degrees), there was no statistical significance found for the IC Amp (R^2 = 0.114, p = 0.338) or IC Imp (R^2 = 0.041, p = 0.202). For eccentricity-5 (12-16 degrees), there was no statistical significance found for the IC Amp (R^2 = 0.028, p = 0.167) or IC Imp (R^2 = 0.014, p = 0.119). For eccentricity-6 (16-20 degrees), there was no statistical significance between AXL and the IC Amp (R^2 = 0.003, p = 0.287) or IC Imp (R^2 = 0.002, p = 0.248).

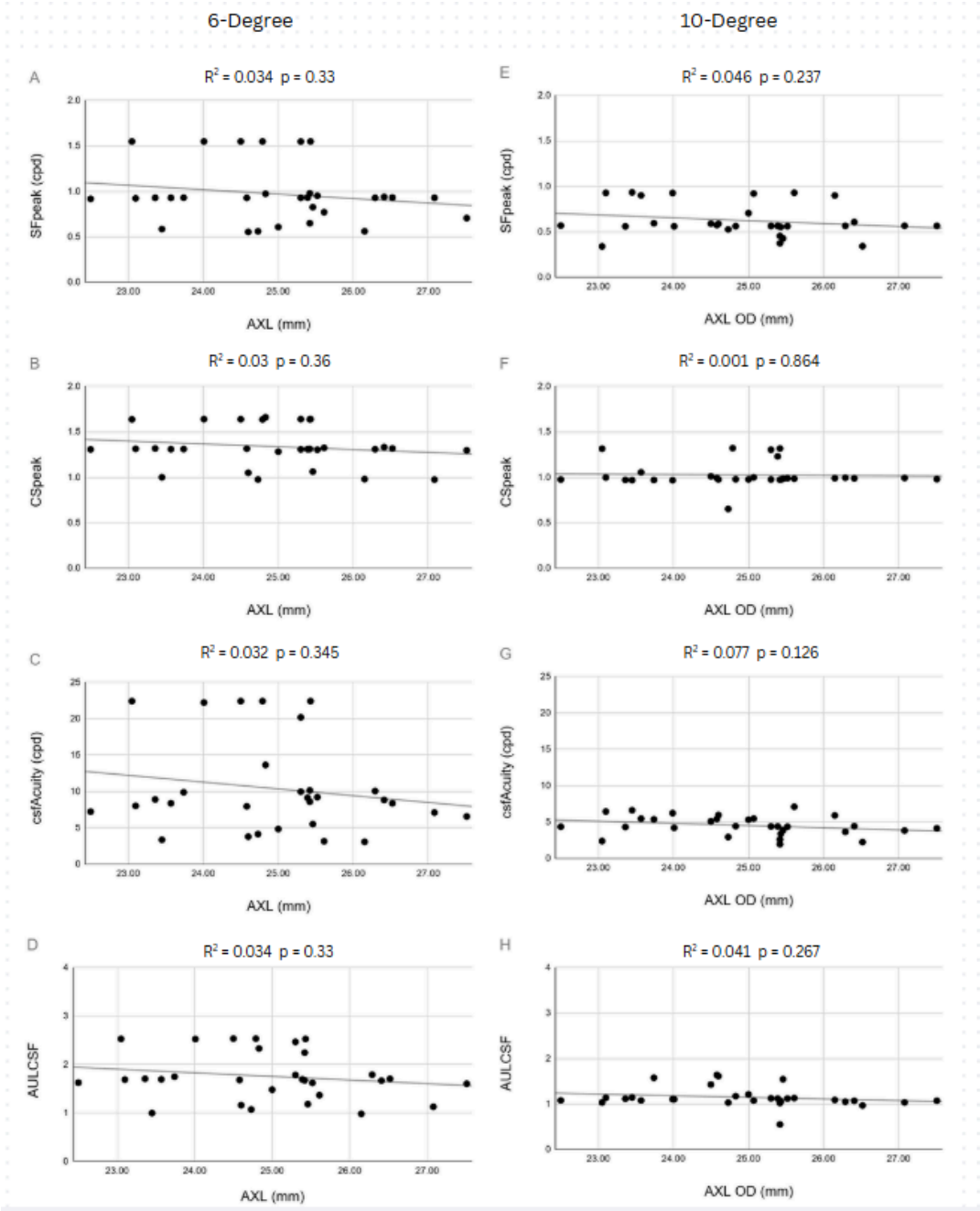

Figure 6. *Peripheral Blue-yellow contrast sensitivity task results. Associated with the koniocellular pathway, with targets centered at 6 and 10 degrees visual angle. The 6 degree centered stimulus peak spatial frequency (A and E), peak contrast sensitivity (B and F), Acuity (C and G), and AULCSF (D and H) plotted against axial length (mm).*

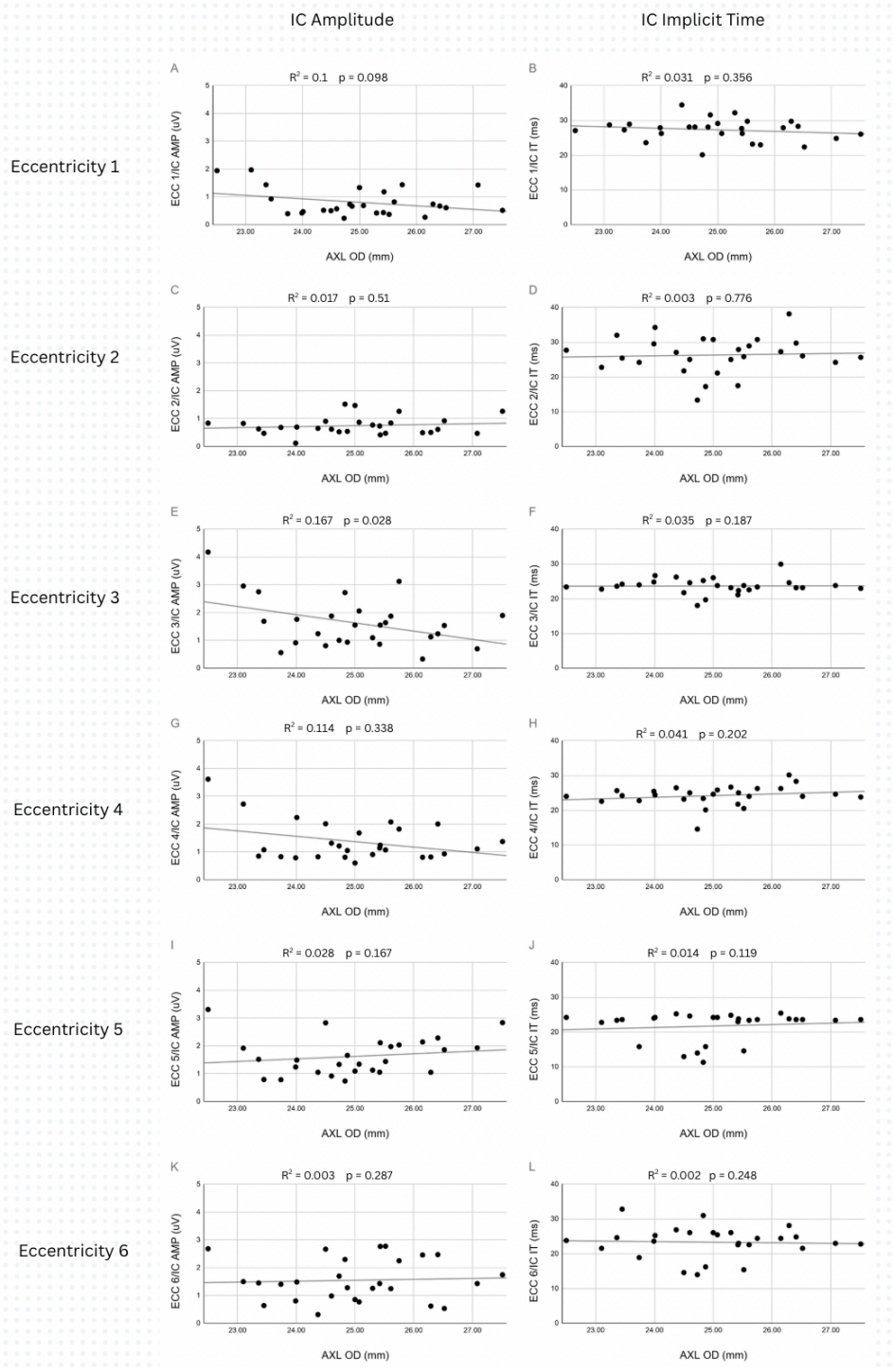

Figure 7. *Global-flash multifocal ERG (GmfERG) results. Eccentricity-1 through 6 from top to bottom, where the left column is IC amplitude (μV) and the right column is IC implicit time (ms) plotted against axial length (mm).*

Comparing the 6- and 10-degrees contrast sensitivity tasks using paired sample T-test, Red-green SFpeak ($p = 1.32 \times 10^{-3}$, $p < 0.005$), CSpeak ($p = 4.21 \times 10^{-11}$, $p < 0.0001$), Acuity ($p = 4.33 \times 10^{-9}$, $p < 0.0001$); Black-white SFpeak ($p = 9.75 \times 10^{-5}$, $p < 0.0001$), CSpeak ($p = 2.18 \times 10^{-4}$, $p < 0.0001$), Acuity ($p = 2.88 \times 10^{-7}$, $p < 0.0001$); Blue-yellow SFpeak ($p = 8.17 \times 10^{-6}$, $p < 0.0001$), CSpeak ($p = 2.30 \times 10^{-8}$, $p < 0.0001$), Acuity ($p = 2.99 \times 10^{-5}$, $p < 0.0001$).

5. Discussion

This cross-sectional study aimed to investigate the functional response of the inner retina, specifically the retinal ganglion cells, in young adults with varying AXLs using both a psychophysical contrast sensitivity test with varying chromatic stimuli and GmfERG. When using a black-white flickering stimulus, the contrast sensitivity task revealed reduced peak spatial frequency with an increased AXL at 6-degrees, whereas an opposite result, increased peak spatial frequency with increasing AXL, was found at 10-degrees eccentricity (Figure 5). This opposite relationship at 6- and 10-degrees retinal eccentricity could point out the role of contrast sensitivity on axial elongation in myopia at specific peripheral locations. Xu et al, 2022 found an increase in contrast sensitivity in young adults with myopia at both 6 and 12 degrees eccentricity, but only in the superior and inferior fields. Note that the current study has not investigated the effect of quadrant on contrast sensitivity. Other studies found a decrease in contrast sensitivity with increasing myopia in the fovea (Liu et al., 2022) or in the far periphery (Kerber et al., 2016; Wang et al., 2024).

The three main types of RGCs differ in size and distribution, which may be influenced by increased AXL, particularly in highly myopic eyes. It is known that with increased AXL, the RGC complex thickness decreases, likely due to the same number of cells occupying a larger area (Hirasawa et al., 2013; Takeyama et al., 2014, Wang et al., 2024). The relative proportion between the different RGCs also differs widely, as midget RGCs make up about 80% of RGCs, with parasol RGCs closer to about 10%, and small-bistratified RGCs making up closer to 8-10% (Edwards et al., 2021). The

different RGCs are not evenly distributed between the three types in terms of size, number, or location. Midget RGCs make up the majority of the RGCs in the retina, but because it is involved in high-acuity vision and detail recognition, they are densest in the central retina, especially in the fovea and parafoveal region (Edwards et al., 2021). Parasol RGCs are much more common in the peripheral retina and are more sparse in the central retina(Edwards et al., 2021). They also have larger receptive fields in comparison to the other two RGCs, with the ratio of parasol to midget cell dendritic field diameter at 3 degrees retinal eccentricity being ~3:1 (Dacey & Petersen, 1992). Midget RGCs and parasol RGCs also have an overlap in the 2-10 degree retinal eccentricity location (Yoonessi & Yoonessi, 2011).

Axial elongation in myopia also likely occurs in a non-uniform manner throughout the eye. Decrease in photoreceptors and retinal pigment epithelium cell density is associated mainly in the retro-equatorial to equatorial regions while choroidal and scleral thinning are more pronounced at the posterior pole vs ora serrata (Jonas et al., 2023). This suggests retinal nerve fibers originating further from the optic nerve would be most affected by axial elongation compared to those more centrally located (Jonas et al., 2023).

Many previous studies have examined the association between the peripheral retina and its role in myopia development in various mammals and humans (Hung et al., 1995; McFadden et al., 2004; Schaeffel et al., 1988). The near peripheral retina has been the focus, as this area is thought to play a crucial role in detecting peripheral defocus, which may influence emmetropization (Smith et al., 2005).

It is important to verify if the contrast sensitivity task is sensitive enough to separate the visual pathways to ensure the validity experiments. All stimuli were significantly different when comparing the 6 and 10-degree eccentricities from the fovea. This shows that the contrast sensitivity test was sensitive enough to detect differences when measuring between the stimulus types at different eccentricities.

This study has several limitations. The first is that the sample size is small. The study originally aimed to recruit 60 subjects, but only achieved around half that. This increased the likelihood of a type II error and possibly misrepresented the wider population. This limitation largely happens due to time constraints while maintaining the four visitation days of the experiment. Another limitation is the difficulty of isolating the specific visual pathways through the contrast sensitivity task. Although the method aimed to target the different pathways individually, there is considerable overlap, particularly between the parvocellular and magnocellular pathways (Edwards et al., 2021). Both pathways contribute to overlapping ranges of spatial frequency, specifically the lower spatial frequencies of the parvocellular pathway and the higher spatial frequencies of the magnocellular pathway. Similarly, there is an overlap in temporal resolution with the magnocellular pathway extending into higher temporal frequencies and the parvocellular pathway contributing to lower temporal frequencies. These overlaps complicate the ability to separate the pathways and may contribute to skewing the results.

The ON-delayed RGCs were newly identified in the mouse retina, which deviates from the normal center-surround configuration (Mani & Schwartz, 2017). As the name

suggests, these RGCs' unusual firing pattern has a much longer latency time comparatively which contributes to its unique function, such as inverted size-latency tuning (responding earlier to larger stimuli) and extra-dendritic activation (activation of RGC beyond the dendritic field) (Mani & Schwartz, 2017). It is possible that with axial elongation that the ON-delayed RGCs, especially with it's extra-dendritic activation, may be affected and is worth studying in the future.

Another important limitation to this study is that we are observing neuronal responses with respect to varying AXL, but we cannot determine whether the observed changes are the cause or consequence of axial elongation. The demographic of this study is all adults with established refractive errors, and thus, it is possible that the observed responses preceded the elongation of the eye. It is recommended to perform a longitudinal study in the future prior to myopia onset to establish response changes with ocular growth.

6. Conclusions

In conclusion, the present study demonstrates that increased ocular AXL is associated with a reduction in acuity and peak contrast sensitivity at this location. These findings, while not fully optimized, suggest that axial elongation in myopia leads to functional changes in the retina at the near periphery. Future research should further investigate the structural changes of ganglion cells at the near periphery using optical coherence tomography (OCT) and whether these changes exist with axial shortening, such as in hyperopes, and further axial elongation. Also, it would be beneficial to do a longitudinal study to observe if the effects precede myopia, or if they are only a consequence of the axial elongation.

7. References

Al-Hashmi, A. M., Kramer, D. J., & Mullen, K. T. (2011). Human vision with a lesion of the parvocellular pathway: An optic neuritis model for selective contrast sensitivity deficits with severe loss of midget ganglion cell function. *Experimental Brain Research*, *215*(3–4), 293–305. https://doi.org/10.1007/s00221-011-2896-4

Alvarez-Peregrina, C., Sánchez-Tena, M. Á., Martinez-Perez, C., & Villa-Collar, C. (2020). The Relationship Between Screen and Outdoor Time With Rates of Myopia in Spanish Children. *Frontiers in Public Health*, *8*, 560378. https://doi.org/10.3389/fpubh.2020.560378

Atchison, D. A., Jones, C. E., Schmid, K. L., Pritchard, N., Pope, J. M., Strugnell, W. E., & Riley, R. A. (2004). Eye shape in emmetropia and myopia. *Investigative Ophthalmology & Visual Science*, *45*(10), 3380–3386. https://doi.org/10.1167/iovs.04-0292

Baden, T., Schaeffel, F., & Berens, P. (2017a). Visual Neuroscience: A Retinal Ganglion Cell to Report Image Focus? *Current Biology: CB*, *27*(4), R139–R141. https://doi.org/10.1016/j.cub.2016.12.022

Baden, T., Schaeffel, F., & Berens, P. (2017b). Visual Neuroscience: A Retinal Ganglion Cell to Report Image Focus? *Current Biology*, *27*(4), R139–R141. https://doi.org/10.1016/j.cub.2016.12.022

Baden, T., Schaeffel, F., & Berens, P. (2017c). Visual Neuroscience: A Retinal Ganglion Cell to Report Image Focus? *Current Biology*, *27*(4), R139–R141. https://doi.org/10.1016/j.cub.2016.12.022

Baird, P. N., Schäche, M., & Dirani, M. (2010). The GEnes in Myopia (GEM) study in understanding the aetiology of refractive errors. *Progress in Retinal and Eye Research*, *29*(6), Article 6. https://doi.org/10.1016/j.preteyeres.2010.05.004

Barbano, L., Ziccardi, L., Antonelli, G., Nicoletti, C. G., Landi, D., Mataluni, G., Falsini, B., Marfia, G. A., Centonze, D., & Parisi, V. (2022). Multifocal Electroretinogram Photopic Negative Response: A Reliable Paradigm to Detect Localized Retinal Ganglion Cells' Impairment in Retrobulbar Optic Neuritis Due to Multiple Sclerosis as a Model of Retinal Neurodegeneration. *Diagnostics*, *12*(5), 1156. https://doi.org/10.3390/diagnostics12051156

Boynton, G. M., Demb, J. B., Glover, G. H., & Heeger, D. J. (1999). Neuronal basis of contrast discrimination. *Vision Research*, *39*(2), 257–269. https://doi.org/10.1016/S0042-6989(98)00113-8

Chen, M., Nofziger, J., Datta, R., Gee, J. C., Morgan, J., & Aguirre, G. K. (2020). The Influence of Axial Length Upon the Retinal Ganglion Cell Layer of the Human Eye. *Translational Vision Science & Technology*, *9*(13), 9. https://doi.org/10.1167/tvst.9.13.9

Chin, M. P., Chu, P. H. W., Cheong, A. M. Y., & Chan, H. H. L. (2015). Human electroretinal responses to grating patterns and defocus changes by global flash multifocal electroretinogram. *PloS One*, *10*(4), e0123480. https://doi.org/10.1371/journal.pone.0123480

Chu, P. H. W., Chan, H. H. L., Ng, Y., Brown, B., Siu, A. W., Beale, B. A., Gilger, B. C., & Wong, F. (2008). Porcine global flash multifocal electroretinogram: Possible mechanisms for the glaucomatous changes in contrast response function. *Vision Research*, *48*(16), 1726–1734. https://doi.org/10.1016/j.visres.2008.05.006

Dacey, D. M., & Petersen, M. R. (1992). Dendritic field size and morphology of midget and parasol ganglion cells of the human retina. *Proceedings of the National Academy of Sciences of the United States of America*, *89*(20), 9666–9670.

Dietze, J., Blair, K., Zeppieri, M., & Havens, S. J. (2025). Glaucoma. In *StatPearls*. StatPearls Publishing. http://www.ncbi.nlm.nih.gov/books/NBK538217/

Edwards, M., Goodhew, S. C., & Badcock, D. R. (2021). Using perceptual tasks to selectively measure magnocellular and parvocellular performance: Rationale and a user's guide. *Psychonomic Bulletin & Review*, *28*(4), 1029–1050. https://doi.org/10.3758/s13423-020-01874-w

Frishman, L., Sustar, M., Kremers, J., McAnany, J. J., Sarossy, M., Tzekov, R., & Viswanathan, S. (2018). ISCEV extended protocol for the photopic negative response (PhNR) of the full-field electroretinogram. *Documenta Ophthalmologica. Advances in Ophthalmology*, *136*(3), 207–211. https://doi.org/10.1007/s10633-018-9638-x

Fung, M. M. Y., Choi, K. Y., & Chan, H. H. L. (2021). The effect of simultaneous dual-focus integration on the global flash multifocal electroretinogram in the human eye. *Ophthalmic & Physiological Optics: The Journal of the British College of Ophthalmic Opticians (Optometrists)*, *41*(1), 171–178. https://doi.org/10.1111/opo.12751

Gottlieb, M. D., Joshi, H. B., & Nickla, D. L. (1990). Scleral changes in chicks with form-deprivation myopia. *Current Eye Research*, *9*(12), 1157–1165. https://doi.org/10.3109/02713689009003472

Hirasawa, K., & Shoji, N. (2013). Association between ganglion cell complex and axial length. *Japanese Journal of Ophthalmology*, *57*(5), 429–434. https://doi.org/10.1007/s10384-013-0241-0

Ho, W., Wong, O., Chan, Y., Wong, S., Kee, C., & Chan, H. H. (2012). Sign-dependent changes in retinal electrical activity with positive and negative defocus in the human eye. *Vision Research*, *52*(1), 47–53. https://doi.org/10.1016/j.visres.2011.10.017

Ho, W.-C., Kee, C.-S., & Chan, H. H.-L. (2012). Myopic children have central reduction in high contrast multifocal ERG response, while adults have paracentral reduction in low contrast response. *Investigative Ophthalmology & Visual Science*, *53*(7), 3695–3702. https://doi.org/10.1167/iovs.11-9379

Hoffmann, M. B., Bach, M., Kondo, M., Li, S., Walker, S., Holopigian, K., Viswanathan, S., & Robson, A. G. (2021). ISCEV standard for clinical multifocal electroretinography (mfERG) (2021 update). *Documenta Ophthalmologica. Advances in Ophthalmology*, *142*(1), 5–16. https://doi.org/10.1007/s10633-020-09812-w

Hogue, W., & Taylor, C. P. (2021). Axial length is associated with individual differences in ON- and OFF- pattern detection. *Investigative Ophthalmology & Visual Science*, *62*(8), 2894.

Holden, B. A., Fricke, T. R., Wilson, D. A., Jong, M., Naidoo, K. S., Sankaridurg, P., Wong, T. Y., Naduvilath, T. J., & Resnikoff, S. (2016). Global Prevalence of Myopia and High Myopia and Temporal Trends from 2000 through 2050. *Ophthalmology*, *123*(5), 1036–1042. https://doi.org/10.1016/j.ophtha.2016.01.006

Hood, D. C., Odel, J. G., Chen, C. S., & Winn, B. J. (2003). The Multifocal Electroretinogram. *Journal of Neuro-Ophthalmology*, *23*(3), 225.

Huang, Y., Chen, X., Zhuang, J., & Yu, K. (2022). The Role of Retinal Dysfunction in Myopia Development. *Cellular and Molecular Neurobiology*, *43*(5), 1905–1930. https://doi.org/10.1007/s10571-022-01309-1

Hung, L.-F., Crawford, M. L. J., & Smith, E. L. (1995). Spectacle lenses alter eye growth and the refractive status of young monkeys. *Nature Medicine*, *1*(8), 761–765. https://doi.org/10.1038/nm0895-761

Irving, E. L., Sivak, J. G., & Callender, M. G. (1992). Refractive plasticity of the developing chick eye. *Ophthalmic and Physiological Optics*, *12*(4), 448–456. https://doi.org/10.1111/j.1475-1313.1992.tb00315.x

Ismael, Z. F., El-Shazly, A. A. E.-F., Farweez, Y. A., & Osman, M. M. M. (2017). Relationship between functional and structural retinal changes in myopic eyes. *Clinical and Experimental Optometry*, *100*(6), 695–703. https://doi.org/10.1111/cxo.12527

Kerber, K. L., Thorn, F., Bex, P. J., & Vera-Diaz, F. A. (2016). Peripheral contrast sensitivity and attention in myopia. *Vision Research*, *125*, 49–54. https://doi.org/10.1016/j.visres.2016.05.004

Kim, U. S., Mahroo, O. A., Mollon, J. D., & Yu-Wai-Man, P. (2021). Retinal Ganglion Cells—Diversity of Cell Types and Clinical Relevance. *Frontiers in Neurology*, *12*, 661938. https://doi.org/10.3389/fneur.2021.661938

Klistorner, A. I. Bm., & Graham, S. L. M. (1999). Early Magnocellular Loss in Glaucoma Demonstrated Using the Pseudorandomly Stimulated Flash Visual Evoked Potential. *Journal of Glaucoma*, *8*(2), 140–148.

Lam, C. S., Edwards, M., Millodot, M., & Goh, W. S. (1999). A 2-year longitudinal study of myopia progression and optical component changes among Hong Kong schoolchildren. *Optometry and Vision Science: Official Publication of the American Academy of Optometry*, *76*(6), 370–380. https://doi.org/10.1097/00006324-199906000-00016

Leonova, A., Pokorny, J., & Smith, V. C. (2003). Spatial frequency processing in inferred PC- and MC-pathways. *Vision Research*, *43*(20), 2133–2139. https://doi.org/10.1016/S0042-6989(03)00333-X

Li, S. Z.-C., Yu, W.-Y., Choi, K.-Y., Lam, C. H.-I., Lakshmanan, Y., Wong, F. S.-Y., & Chan, H. H.-L. (2017). Subclinical Decrease in Central Inner Retinal Activity Is Associated With Myopia Development in Children. *Investigative Ophthalmology & Visual Science*, *58*(10), 4399–4406. https://doi.org/10.1167/iovs.16-21279

Liu, X., Wang, Y., Ying, X., Zhang, F., Huang, J., Yu, H., Wang, Q., Zheng, M., Hou, F., Lesmes, L., Lu, Z.-L., Lu, F., & Mao, X. (2022). Contrast Sensitivity Is Associated With Chorioretinal Thickness and Vascular Density of Eyes in Simple Early-Stage High Myopia. *Frontiers in Medicine*, *9*. https://doi.org/10.3389/fmed.2022.847817

Ma, Y., Wen, Y., Zhong, H., Lin, S., Liang, L., Yang, Y., Jiang, H., Chen, J., Huang, Y., Ying, X., Resnikoff, S., Lu, L., Zhu, J., Xu, X., He, X., & Zou, H. (2022). Healthcare utilization and economic burden of myopia in urban China: A nationwide cost-of-illness study. *Journal of Global Health*, *12*, 11003. https://doi.org/10.7189/jogh.12.11003

Mani, A., & Schwartz, G. W. (2017). Circuit mechanisms of a retinal ganglion cell with stimulus dependent response latency and activation beyond its dendrites. *Current Biology : CB*, *27*(4), 471–482. https://doi.org/10.1016/j.cub.2016.12.033

McFadden, S. A., Howlett, M. H. C., & Mertz, J. R. (2004). Retinoic acid signals the direction of ocular elongation in the guinea pig eye. *Vision Research*, *44*(7), 643–653. https://doi.org/10.1016/j.visres.2003.11.002

Pan, C.-W., Ramamurthy, D., & Saw, S.-M. (2012). Worldwide prevalence and risk factors for myopia. *Ophthalmic and Physiological Optics*, *32*(1), 3–16. https://doi.org/10.1111/j.1475-1313.2011.00884.x

Rose, K., Harper, R., Tromans, C., Waterman, C., Goldberg, D., Haggerty, C., & Tullo, A. (2000). Quality of life in myopia. *The British Journal of Ophthalmology*, *84*(9), 1031–1034. https://doi.org/10.1136/bjo.84.9.1031

Saw, S.-M., Gazzard, G., Shih-Yen, E. C., & Chua, W.-H. (2005). Myopia and associated pathological complications. *Ophthalmic & Physiological Optics: The Journal of the British College of Ophthalmic Opticians (Optometrists)*, *25*(5), 381–391. https://doi.org/10.1111/j.1475-1313.2005.00298.x

Schaeffel, F., Glasser, A., & Howland, H. C. (1988). Accommodation, refractive error and eye growth in chickens. *Vision Research*, *28*(5), 639–657. https://doi.org/10.1016/0042-6989(88)90113-7

Sezgin Akcay, B. I., Gunay, B. O., Kardes, E., Unlu, C., & Ergin, A. (2017). Evaluation of the Ganglion Cell Complex and Retinal Nerve Fiber Layer in Low, Moderate, and High Myopia: A Study by RTVue Spectral Domain Optical Coherence Tomography. *Seminars in Ophthalmology*, *32*(6), 682–688. https://doi.org/10.3109/08820538.2016.1170157

Shimada, Y., Bearse, M. A., & Sutter, E. E. (2005). Multifocal electroretinograms combined with periodic flashes: Direct responses and induced components. *Graefe's Archive for Clinical and Experimental Ophthalmology*, *243*(2), 132–141. https://doi.org/10.1007/s00417-004-1072-y

Smith, E. L., Kee, C., Ramamirtham, R., Qiao-Grider, Y., & Hung, L.-F. (2005). Peripheral Vision Can Influence Eye Growth and Refractive Development in Infant Monkeys. *Investigative Ophthalmology & Visual Science*, *46*(11), 3965–3972. https://doi.org/10.1167/iovs.05-0445

Stoimenova, B. D. (2007). The Effect of Myopia on Contrast Thresholds. *Investigative Ophthalmology & Visual Science*, *48*(5), 2371–2374. https://doi.org/10.1167/iovs.05-1377

Tanaka, H., Ishida, K., Ozawa, K., Ishihara, T., Sawada, A., Mochizuki, K., & Yamamoto, T. (2021). Relationship between structural and functional changes in glaucomatous eyes: A multifocal electroretinogram study. *BMC Ophthalmology*, *21*(1), 305. https://doi.org/10.1186/s12886-021-02061-8

Troilo, D., Gottlieb ,Michael D., & and Wallman, J. (1987). Visual deprivation causes myopia in chicks with optic nerve section. *Current Eye Research*, *6*(8), 993–999. https://doi.org/10.3109/02713688709034870

Troilo, D., Smith, E. L., Nickla, D. L., Ashby, R., Tkatchenko, A. V., Ostrin, L. A., Gawne, T. J., Pardue, M. T., Summers, J. A., Kee, C., Schroedl, F., Wahl, S., & Jones, L. (2019). IMI – Report on Experimental Models of Emmetropization and Myopia. *Investigative Ophthalmology & Visual Science*, *60*(3), M31–M88. https://doi.org/10.1167/iovs.18-25967

Turnbull, P. R. K., Goodman, L. K., & Phillips, J. R. (2020). Global-flash mfERG responses to local differences in spherical and astigmatic defocus across the human retina. *Ophthalmic and Physiological Optics*, *40*(1), 24–34. https://doi.org/10.1111/opo.12656

Van Alstine, A. W., & Viswanathan, S. (2017). Test–retest reliability of the multifocal photopic negative response. *Documenta Ophthalmologica*, *134*(1), 25–36. https://doi.org/10.1007/s10633-016-9569-3

Wen, L., Cao, Y., Cheng, Q., Li, X., Pan, L., Li, L., Zhu, H., Lan, W., & Yang, Z. (2020). Objectively measured near work, outdoor exposure and myopia in children. *The British*

Journal of Ophthalmology, *104*(11), 1542–1547. https://doi.org/10.1136/bjophthalmol-2019-315258

Westall, C. A., Dhaliwal, H. S., Panton, C. M., Sigesmund, D., Levin, A. V., Nischal, K. K., & Héon, E. (2001). Values of electroretinogram responses according to axial length. *Documenta Ophthalmologica*, *102*(2), 115–130. https://doi.org/10.1023/A:1017535207481

Wild, J. M. (2001). Short wavelength automated perimetry. *Acta Ophthalmologica Scandinavica*, *79*(6), 546–559. https://doi.org/10.1034/j.1600-0420.2001.790602.x

Xu, Z., Zhuang, Y., Chen, Z., Hou, F., Chan, L. Y. L., Feng, L., Ye, Q., He, Y., Zhou, Y., Jia, Y., Yuan, J., Lu, Z.-L., & Li, J. (2022). Assessing the contrast sensitivity function in myopic parafovea: A quick contrast sensitivity functions study. *Frontiers in Neuroscience*, *16*, 971009. https://doi.org/10.3389/fnins.2022.971009

Ye, Q., Xu, K., Chen, Z., Liu, Z., Fan, Y., Liu, P., Yu, M., & Yang, Y. (2024). Early impairment of magnocellular visual pathways mediated by isolated-check visual evoked potentials in primary open-angle glaucoma: A cross-sectional study. *BMJ Open Ophthalmology*, *9*(1), e001463. https://doi.org/10.1136/bmjophth-2023-001463

Yoonessi, A., & Yoonessi, A. (2011). Functional Assessment of Magno, Parvo and Konio-Cellular Pathways; Current State and Future Clinical Applications. *Journal of Ophthalmic & Vision Research*, *6*(2), 119–126.